Nonequilibrium Fluctuations and Enhanced Diffusion of a Driven Particle in a Dense Environment

Pierre Illien,[1,2*] Olivier Bénichou,[3] Gleb Oshanin,[3] Alessandro Sarracino,[4,5] and Raphaël Voituriez[3,6]
[1]*Rudolf Peierls Centre for Theoretical Physics, University of Oxford, Oxford OX1 3NP, United Kingdom*
[2]*Department of Chemistry, The Pennsylvania State University, University Park, Pennsylvania 16802, USA*
[3]*Laboratoire de Physique Théorique de la Matière Condensée, CNRS UMR 7600, Université Pierre-et-Marie-Curie, 4 Place Jussieu, 75005 Paris, France*
[4]*Istituto dei Sistemi Complessi-CNR, P.le Aldo Moro 2, 00185 Rome, Italy*
[5]*Dipartimento di Fisica, Università di Roma Sapienza, P.le Aldo Moro 2, 00185 Rome, Italy*
[6]*Laboratoire Jean Perrin, CNRS UMR 8237, Université Pierre-et-Marie-Curie, 4 Place Jussieu, 75005 Paris, France*

(Received 18 July 2017; revised manuscript received 2 January 2018; published 16 May 2018)

We study the diffusion of a tracer particle driven out of equilibrium by an external force and traveling in a dense environment of arbitrary density. The system evolves on a discrete lattice and its stochastic dynamics is described by a master equation. Relying on a decoupling approximation that goes beyond the naive mean-field treatment of the problem, we calculate the fluctuations of the position of the tracer around its mean value on a lattice of arbitrary dimension, and with different boundary conditions. We reveal intrinsically nonequilibrium effects, such as enhanced diffusivity of the tracer induced by both the crowding interactions and the external driving. We finally consider the high-density and low-density limits of the model and show that our approximation scheme becomes exact in these limits.

DOI: 10.1103/PhysRevLett.120.200606

Introduction.—Biased diffusion in crowded media is ubiquitous in living systems. At the molecular level, biological motors are able to overcome thermal fluctuations to achieve directed motion and perform highly precise functions. At the cellular level, bacteria are able to self-propel within densely packed biofilms. Both examples involve a biased, or more generally persistent particle that moves in a directed manner, and a crowded environment. The description of such systems constitutes a key problem of modern statistical physics [1,2]. Beyond fundamental interests, understanding the transport and diffusion properties of biased particles in complex environments finds applications in the field of artificial active matter [3,4] and in active microrheology [5–7]. The interplay between the dynamics of the active agents and their passive surroundings can trigger self-assembly, through effective interactions mediated by the quiescent medium [8–11].

Recently, from an analytical perspective, the question of the diffusion of a biased particle, i.e., the limit case of an active particle with infinite persistence, which interacts with a bath of passive particles, has received growing interest through different approaches [12,13]. Here, we focus on the case where the particles interact via hard-core interactions and evolve on a lattice. This model is a variation on exclusion processes, which are paradigmatic models of nonequilibrium statistical mechanics [2,14]. In the generic situation where the lattice dimension is greater than one and where the density of particles is arbitrary, results are essentially limited to the *mean displacement* of the tracer [15–18]. The *fluctuations* of the tracer position around its mean value received less interest, and results are limited to the case of *fixed* obstacles at low density [19], or for *mobile* obstacles at high density [20]. Crucially, the fluctuations of the tracer position actually contain information about the environment of the system and its nonequilibrium dynamics, as illustrated by the studies of the diffusion of driven particles in supercooled liquids close to the glass transition [21,22], in biased periodic potentials [23–25], disordered systems [26], or for active particles [27]. Actually, the problem where the tracer is not biased is already highly complex and does not admit an exact solution, although an approximate yet very accurate expression of the diffusion coefficient as a function of the bath density in 2D was found by Nakazato and Kitahara [28].

In this Letter, we calculate the fluctuations of the position of the driven tracer around its mean value in the generic case of a bath of arbitrary density and on lattices of dimension 2 and 3, which constitute the most physically relevant situations. Our analytical approximations are valid both when the system is infinite in every direction and when it is confined in directions perpendicular to the applied bias. Monte Carlo simulations of the master equation confirm the accuracy of our closure scheme. Remarkably, our approach reveals that the diffusion of the tracer can be maximized, either as a function of the driving force or as a function of the density of bath particles. We emphasize that these effects cannot be

predicted within a linear-response description. We finally show that our approximate expression becomes *exact* in the high- and low-density limits, which highlights the consistency and relevance of our closure scheme.

Model.—We consider the general problem of a biased tracer in a dynamic environment, i.e., with mobile obstacles of density ρ. The bath particles and the tracer evolve on a cubic lattice, of spacing σ and of arbitrary dimension d, that can be infinite in every direction or finite with periodic boundary conditions in the directions perpendicular to the bias. The bath particles perform symmetric random walks, and jump on adjacent sites with rate $1/(2d\tau^*)$. The tracer performs a biased random walk, and jumps in direction ν with rate p_ν/τ. We assume hard-core (exclusion) interactions between all the particles present on the lattice. The set of jump probabilities $\{p_\nu\}$ is *a priori* arbitrary. However, it can be convenient to assume that the bias is controlled by an external force $\boldsymbol{F} = F\boldsymbol{e}_1$, and that $p_\nu = \exp(\boldsymbol{F}\cdot\boldsymbol{e}_\nu/2)/Z$, where $Z = \sum_\mu \exp(\boldsymbol{F}\cdot\boldsymbol{e}_\mu/2)$ is a normalization constant and $\boldsymbol{e}_\mu$ are the base vectors of the lattice (sums on greek letter indices run implicitly on $\{\pm1,\ldots,\pm d\}$).

Analytical approximation.—The state of the system at a given time is described by the position of the tracer $\boldsymbol{X}$ and the configuration of the lattice $\eta = \{\eta_{\boldsymbol{r}}\}$, where $\eta_{\boldsymbol{r}} = 1$ if site $\boldsymbol{r}$ is occupied by a bath particle and 0 otherwise. Enumerating the possible configurations of the system, one can write the master equation satisfied by the probability distribution $P(\boldsymbol{X},\eta;t)$ under the form

$$\partial_t P(\boldsymbol{X},\eta;t) = \mathcal{L}_{\text{bath}}P + \mathcal{L}_{\text{TP}}P, \tag{1}$$

where the terms in the rhs describe, respectively, the symmetric diffusion of bath particles and the biased diffusion of the tracer particle (TP) constrained by hard-core interactions. The expression of these operators is given in the Supplemental Material (SM) [29]. The evolution equation for the mean displacement of the tracer can be deduced from the master equation [Eq. (1)], and was described in previous publications [18,30]. We recall it in the SM [29]. We focus here on the variance of the tracer position in the direction of the bias, defined as

$$\sigma_X^2(t) \equiv \langle [X_t - \langle X_t\rangle]^2\rangle = \langle {X_t}^2\rangle - \langle X_t\rangle^2, \tag{2}$$

and whose evolution equation is obtained straightforwardly by multiplying Eq. (1) by $(\boldsymbol{X}\cdot\boldsymbol{e}_1)$ and $(\boldsymbol{X}\cdot\boldsymbol{e}_1)^2$ and summing over all configurations $\boldsymbol{X}$ and η:

$$\frac{d}{dt}\sigma_X^2(t) = -\frac{2\sigma}{\tau}[p_1\tilde{g}_{\boldsymbol{e}_1}(t) - p_{-1}\tilde{g}_{\boldsymbol{e}_{-1}}(t)] + \frac{\sigma^2}{\tau}\{p_1[1-k_{\boldsymbol{e}_1}(t)] + p_{-1}[1-k_{\boldsymbol{e}_{-1}}(t)]\}, \tag{3}$$

which holds in dimensions greater than 1, and where we define the density profiles $k_{\boldsymbol{r}} \equiv \langle\eta_{\boldsymbol{r}}\rangle$ and the correlation functions $\tilde{g}_{\boldsymbol{r}} \equiv \langle(X_t - \langle X_t\rangle)(\eta_{\boldsymbol{r}} - \langle\eta_{\boldsymbol{r}}\rangle)\rangle$ that couple the dynamics of the tracer with that of the bath of particles, and where $\boldsymbol{r}$ is evaluated in the frame of reference of the tracer. The diffusion coefficient of the tracer particle, defined as $D \equiv (1/2d)\lim_{t\to\infty}(d/dt)\sigma_X^2(t)$, can be deduced straightforwardly from Eq. (3).

The evolution equations of the density profiles $k_{\boldsymbol{r}}$ and of the cross-correlation functions $\tilde{g}_{\boldsymbol{r}}$ involve higher-order cross-correlation functions, and the infinite hierarchy of equations yielded by the master equation can be closed by the following mean-field-type decoupling approximations:

$$\langle\eta_{\boldsymbol{r}}\eta_{\boldsymbol{r}'}\rangle \simeq \langle\eta_{\boldsymbol{r}}\rangle\langle\eta_{\boldsymbol{r}'}\rangle, \tag{4}$$

$$\langle\delta X_t\eta_{\boldsymbol{r}}\eta_{\boldsymbol{r}'}\rangle \simeq \langle\eta_{\boldsymbol{r}}\rangle\langle\delta X_t\eta_{\boldsymbol{r}'}\rangle + \langle\eta_{\boldsymbol{r}'}\rangle\langle\delta X_t\eta_{\boldsymbol{r}}\rangle, \tag{5}$$

obtained by writing each random variable x as $x = \langle x\rangle + \delta x$ and neglecting terms of order $\mathcal{O}(\delta x^2)$ [Eq. (4)] and $\mathcal{O}(\delta x^3)$ [Eq. (5)]. We emphasize here that these approximations go beyond naive mean field, as the density profiles $\langle\eta_{\boldsymbol{r}}\rangle$ are not replaced by their spatial average ρ. This closure scheme yields closed evolution equations for the density profiles and cross-correlation functions [31]. Noticing that $\lim_{|\boldsymbol{r}|\to\infty}k_{\boldsymbol{r}} = \rho$, i.e., the density profiles relax to their spatial average far from the tracer, we define the quantities $h_{\boldsymbol{r}} = k_{\boldsymbol{r}} - \rho$ and will use the notation $h_\mu \equiv h_{\boldsymbol{e}_\mu}$.

Using discrete Fourier transforms [29], we find that, in the stationary limit $t\to\infty$, the density profiles $h_{\boldsymbol{r}}$ and the cross-correlation functions $\tilde{g}_{\boldsymbol{r}}$ obey the equations

$$\mathcal{A}h_{\boldsymbol{r}} = \sum_\nu A_\nu h_\nu \nabla_{-\nu}\mathcal{F}_{\boldsymbol{r}} - \rho(A_1 - A_{-1})(\nabla_1 - \nabla_{-1})\mathcal{F}_{\boldsymbol{r}}, \tag{6}$$

$$\tilde{g}_{\boldsymbol{r}} = \frac{1}{\mathcal{A}}\left\{\sum_\mu\left(A_\mu - \frac{2d\tau^*}{\tau}p_\mu h_\mu\right)\tilde{g}_\mu\nabla_{-\mu} + \frac{2d\tau^*}{\tau}\left[\rho\sum_{\epsilon=\pm1}\epsilon p_\epsilon\tilde{g}_\epsilon(\nabla_1 - \nabla_{-1}) - \sigma\sum_{\epsilon=\pm1}\epsilon p_\epsilon(1-\rho-h_\epsilon)[\rho(\nabla_\epsilon + 1) + h_\epsilon]\right]\right\}\mathcal{F}_{\boldsymbol{r}} - \frac{2d\tau^*}{\tau}\frac{1}{\mathcal{A}^2}\left\{\sum_\mu A_\mu h_\mu\nabla_{-\mu} - \rho(A_1 - A_{-1})(\nabla_1 - \nabla_{-1})\right\}\left\{\sum_\mu p_\mu\tilde{g}_\mu\nabla_\mu - \sigma\sum_{\epsilon=\pm1}\epsilon p_\epsilon(1-\rho-h_\epsilon)\nabla_\epsilon\right\}\mathcal{G}_{\boldsymbol{r}}, \tag{7}$$

where we define the discrete gradient operators $\nabla_\mu f_{\boldsymbol{r}} \equiv f_{\boldsymbol{r}+\boldsymbol{e}_\mu} - f_{\boldsymbol{r}}$, the coefficients

$$A_\nu \equiv \frac{1 + \frac{2d\tau^*}{\tau} p_\nu (1-\rho-h_\nu)}{\sum_\mu [1 + \frac{2d\tau^*}{\tau} p_\mu (1-\rho-h_\mu)]}, \tag{8}$$

and their sum $\mathcal{A} = \sum_\mu A_\mu$. The functions $\mathcal{F}_{\boldsymbol{r}}$ are defined as the limits $\mathcal{F}_{\boldsymbol{r}} = \lim_{\xi\to 1} \hat{\mathcal{P}}(\boldsymbol{r}|\boldsymbol{0};\xi)$, where $\hat{\mathcal{P}}(\boldsymbol{r}|\boldsymbol{0};\xi)$ is the generating function associated with the propagator of a random walk starting from $\boldsymbol{0}$ and arriving at site $\boldsymbol{r}$ on a d-dimensional lattice with the following evolution rules: the random walk goes in direction -1 with probability $A_1/\mathcal{A}$, in direction 1 with probability $A_{-1}/\mathcal{A}$, and in any other direction with probability $A_2/\mathcal{A}$. In what follows, we will consider two types of lattices: (i) d-dimensional lattices infinite in every direction and (ii) generalized capillarylike lattices, infinite in the direction of the applied bias and finite (of size L) with periodic boundary conditions in all the other directions. The Fourier transform of $\hat{\mathcal{P}}(\boldsymbol{r}|\boldsymbol{0};\xi)$ is simply given by $\tilde{\hat{\mathcal{P}}}(\boldsymbol{q};\xi) = [1 - \xi\lambda(\boldsymbol{q})]^{-1}$, where λ is the structure function of this random walk [29,32]. We finally define $\mathcal{G}_{\boldsymbol{r}} = \lim_{\xi\to 1}(\partial/\partial\lambda)\hat{\mathcal{P}}(\boldsymbol{r}|\boldsymbol{0};\xi)$. We emphasize the generality of Eqs. (6) and (7), that hold for different lattice geometries (infinite or bounded), which only affect the expression of the generating functions $\hat{\mathcal{P}}$ [29].

The determination of D requires the knowledge of $h_{\pm 1}$ and $\tilde{g}_{\pm 1}$ [see Eq. (3)]. Although Eqs. (6) and (7) cannot be solved explicitly, $h_{\pm 1}$ and $\tilde{g}_{\pm 1}$ can be determined using a numerical procedure that we sketch here, with further details to be found in the SM [29]. The first step consists in noticing that Eq. (6) evaluated for $\boldsymbol{r} = \boldsymbol{e}_1, \boldsymbol{e}_{-1}$ and $\boldsymbol{e}_2$ yields a closed set of three equations for h_1, h_{-1}, and h_2, where we have used that $h_\mu = h_2$ for $\mu = \pm 2, \ldots, \pm d$ for symmetry reasons, and the explicit expressions of A_ν [Eq. (8)] and $\mathcal{F}_{\boldsymbol{r}}$ [Eq. (S24) of SM [29]]. This system is solved numerically for any set of parameters. Next, Eq. (7) is written for $\boldsymbol{r} = \boldsymbol{e}_1, \boldsymbol{e}_{-1}$ and $\boldsymbol{e}_2$, which, now that h_1, h_{-1}, and h_2 are known, provides a closed set of three equations for $\tilde{g}_1$, $\tilde{g}_{-1}$, and $\tilde{g}_2$. Using the explicit expression of $\mathcal{G}_{\boldsymbol{r}}$ [Eq. (S25) of SM [29]], this set of equations can be solved numerically. Finally, this determines $h_{\pm 1}$ and $\tilde{g}_{\pm 1}$, and allows us to plot the diffusion coefficient D against the different variables (density, force).

Equations (6) and (7), together with the evolution equation of the variance $\sigma_X^2(t)$ [Eq. (3)], constitute the central result of this Letter. Using exact Monte Carlo samplings of the master equation, the approximations obtained from our decoupling scheme are shown to be extremely accurate for a wide range of parameters. Moreover, we show below that our equations yield the exact expressions of the fluctuations of the tracer position in the high- and low-density limits. We also note that, in the absence of bias, our expression reduces to that obtained by Nakazato and Kitahara [28]. From this point of view, our approach constitutes a nonequilibrium extension of that key result. It allows us to unveil typically nonequilibrium effects with respect to both the density and the bias experienced by the tracer.

Crowding-induced enhanced diffusion.—Using Eqs. (6) and (7), we first study the behavior of D as a function of the particle density ρ, at fixed external force F. As shown in Fig. 1, which confronts our analytical approximation with Monte Carlo simulations of the master equation, a nonmonotonic behavior is observed for large enough forces. This means that, counterintuitively, the diffusivity of the biased tracer can actually be enhanced by the addition of passive particles on the lattice. To gain insight into this nontrivial behavior, we consider separately the different contributions in the expression of the fluctuations of the tracer position [Eq. (3)]. While the contribution to the diffusion coefficient involving the density profiles [defined as $K \equiv (\sigma^2/4\tau)[p_1(1-k_{\boldsymbol{e}_1}) + p_{-1}(1-k_{\boldsymbol{e}_{-1}})]$] and the contribution involving the function $\tilde{g}_{\boldsymbol{e}_{-1}}$ are systematically monotonic (decreasing) functions of the density [Fig. 1(e)], the contribution involving the cross-correlation $\tilde{g}_{\boldsymbol{e}_1}$ becomes nonmonotonic for large enough forces [Fig. 1(f)]. This shows that crowding-induced enhanced diffusion originates from

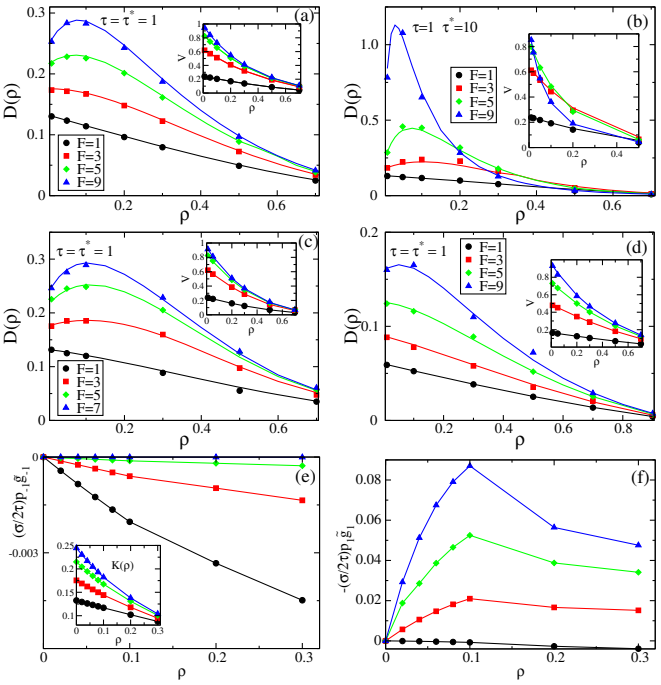

FIG. 1. (a)–(d) Comparison between analytical approximations (lines) for $D(\rho)$ and numerical simulations (symbols). (a) 2D infinite lattice, $\tau = \tau^* = 1$. (b) 2D infinite lattice, $\tau = 1$, $\tau^* = 10$. (c) Quasi-1D striplike lattice of width $L = 3$, with $\tau = \tau^* = 1$. (d) 3D infinite lattice, $\tau = \tau^* = 1$. The approximation is very accurate in a wide range of parameters. In each plot, the inset shows the velocity of the tracer particle as a function of the density. (e),(f) Contributions (analytical approximations) to $D(\rho)$ on a 2D lattice that involve the cross-correlation function $\tilde{g}_1$ (e), $\tilde{g}_{-1}$ (f) and the density profiles [inset of (e)] for the values of F given in (a).

cross-correlations between the position of the tracer and the occupation of the site located immediately ahead in the direction of the force, which become more pronounced for an increasing driving force.

Force-induced enhanced diffusion.—We also study the dependence of D on the external force, keeping the total density ρ fixed. In this case, for large enough values of τ^* (the typical waiting time of bath particles between two moves), a nonmonotonic behavior of the diffusion coefficient as a function of F is found (Fig. 2). This means that there exists an optimal value of the external force which produces the maximum of diffusivity. This kind of behavior is similar to the negative differential mobility observed in analogous models [17,18,30,34] (see inset of Fig. 2). Although increasing the driving force reduces the travel time of the tracer between consecutive obstacles, it will increase the time the tracers spends trapped by bath particles if they are slow enough. The trade-off between these two competing effects results in a nonmonotonic dependence of the diffusion coefficient as a function of the driving force, and to the existence of an optimum diffusivity. Force-induced enhanced diffusion and negative mobility are found to be related, although the effect is more pronounced for the velocity. For all tested values of parameters, the velocity $V(F)$ and the diffusion coefficient $D(F)$ have the same monotonicity as a function of F. Note that, on the contrary, crowding-induced enhanced diffusion occurs while the velocity is always decreasing with the density.

High-density limit.—The high-density limit of the problem can be studied exactly by relating the statistical properties of the tracer position to the first-passage densities of the vacancies (empty sites on the lattice) [35–37]. At linear order in $(1-\rho)$, i.e., when the vacancies have independent dynamics, explicit expressions for the fluctuations of the tracer position have been obtained [20]. In confined systems, this analysis revealed the existence of a transient regime in which the fluctuations of the tracer position are superdiffusive, growing as $t^{3/2}$ on generalized capillaries and as $t \ln t$ on an infinite two-dimensional lattice. The tracer ultimately reaches a regular diffusive regime, after a crossover time that scales as $1/(1-\rho)^2$, in such a way that the superdiffusive fluctuations can be long-lived for crowded systems. Importantly, these results can be retrieved using Eqs. (6) and (7).

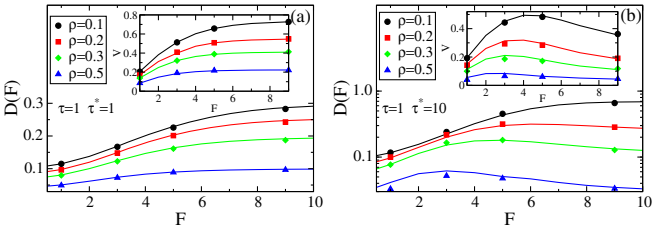

FIG. 2. Comparison between analytical approximations (lines) and numerical simulations (symbols) for $D(F)$ and $V(F)$ (inset), for $\tau = \tau^* = 1$ (a) and $\tau = 1$ and $\tau^* = 10$ (b), for different values of ρ in a 2D infinite lattice. Note the nonmonotonic behavior of $D(F)$ for $\tau^* = 10$ [33].

First, the transient regime can be obtained by taking the limit $\rho \to 1$ and then the long-time limit $t \to \infty$ of the evolution equations for $k_{\boldsymbol{r}}$ and $\tilde{g}_{\boldsymbol{r}}$ [29]. Using generic relations for propagators on lattice random walks to simplify the combinations of $\mathcal{F}_{\boldsymbol{r}}$ [29,32], we obtain the asymptotic expression for the fluctuations of the tracer, which coincides with the exact expressions [20]:

$$\sigma_X^2(t) \sim \sigma^2(1-\rho)\begin{cases} \frac{8a_0^2}{3L^{d-1}}\sqrt{\frac{d}{2\pi}}t^{3/2} & d \text{ capillaries} \\ \frac{2a_0^2}{\pi} t \ln t & \text{2D lattice,} \end{cases} \tag{9}$$

where we define $a_0 = (p_1 - p_{-1})/[1 + 2d\alpha(p_1 + p_{-1})/(2d - \alpha)]$. Note that we considered for simplicity the case where $\tau = \tau^*$, which corresponds to the discrete vacancy-mediated dynamics described above. The coefficient α depends on the geometry of the lattice through the relation $\alpha = \lim_{\xi \to 1}[\hat{P}(\mathbf{0}|\mathbf{0};\xi) - \hat{P}(2\boldsymbol{e}_1|\mathbf{0};\xi)]$, where $\hat{P}(\boldsymbol{r}|\boldsymbol{r}_0;\xi)$ is the generating function of a symmetric random walk starting from $\boldsymbol{r}_0$ and arriving at $\boldsymbol{r}$ on the considered lattice.

The ultimate diffusive regime is obtained by taking $t \to \infty$ first and ultimately $\rho \to 1$. In the high-density limit, Eqs. (6) and (7) reduce to linear systems that can be solved explicitly [29]. We finally obtain

$$\sigma_X^2(t) \sim \begin{cases} \frac{2\sigma^2}{L^{d-1}}\left[\frac{1}{a_0} + \frac{4d^2}{L^{d-1}(2d-\alpha)}\right]^{-1} t & d \text{ capillaries} \\ \frac{4\sigma^2 a_0^2}{\pi}(1-\rho)\ln(\frac{1}{1-\rho})t & \text{2D lattice.} \end{cases} \tag{10}$$

The asymptotic expressions of the fluctuations of the tracer position presented in Eqs. (9) and (10) then coincide with the results obtained from the exact approach [20]. This shows that the decoupling approximation [Eqs. (4) and (5)] we propose to treat the master equation of the problem is exact in the high-density limit.

Low-density limit.—Finally, we consider the low-density limit of our decoupling approximation. In this limit, the rescaled density profiles can be expanded as $h_\nu = v_\nu \rho + \mathcal{O}(\rho^2)$, where the coefficients v_ν (for $\nu = \pm 1, 2$) are the solution of a linear set of three equations [30]. By taking the limit of $\rho \to 0$ of Eq. (7), we extend this result to the cross-correlation functions $\tilde{g}$ that read $\tilde{g}_\nu = u_\nu \rho + \mathcal{O}(\rho^2)$, where the coefficients u_ν are the solution of another set of linear equations [29]. The asymptotic expression of the diffusion coefficient D in two dimensions coincides numerically with the exact analytical solutions in the limit of fixed obstacles ($\tau^* \to \infty$), that reveal a nonanalytic behavior at small forces and an exponential divergence at large forces [see Eqs. (16) and (17) in Ref. [19]]. We find an excellent agreement between our result from the decoupling approximation and the exact expression, as shown in Fig. 3. This additional

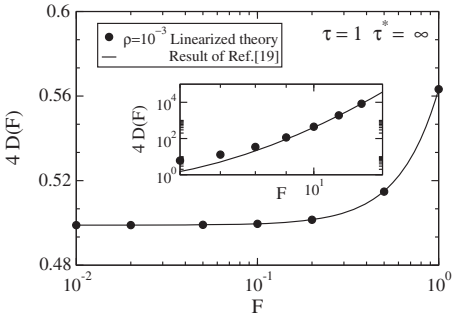

FIG. 3. Comparison between the result of Ref. [19] for small forces and large forces (inset) and the result from our linearized approximation in a 2D infinite lattice with fixed obstacles.

comparison strongly suggests that our decoupling approximation is exact in both the high- and low-density limit. We expect this result to hold when the obstacles can move ($\tau^* < \infty$), as the decoupling approximation works best when the environment of the tracer is mobile. As a by-product of our approach, we thus obtained an exact expression for the diffusion coefficient of the tracer in the low-density limit.

Conclusion.—In this Letter, we studied the statistical properties of a biased random walker traveling in a passive bath of particles on a lattice of dimension 2 or more. The master equation of the problem is solved through a decoupling scheme that goes beyond a naive mean-field approximation, and we calculate the fluctuations of the position of the tracer particle for an arbitrary set of parameters. We reveal striking counterintuitive and intrinsically nonequilibrium effects, namely crowding-induced and force-induced enhanced diffusion. The force-enhanced diffusion is related to the phenomenon of negative differential mobility [18,30]: although increasing the applied force on the tracer can reduce its travel time between different obstacles, it will increase the time it spends trapped by the bath particles if they move sufficiently slowly. The competition between these two effects is at the origin of the nonmonotonic behavior of the diffusion coefficient of the tracer particle. The effect of density-enhanced diffusion is more subtle and relies on nontrivial cross-correlations between the tracer and the bath particles. By studying the different contributions to the diffusion coefficient that are unveiled by our analytical approach, we show that crowding-induced enhanced diffusion originates from the cross-correlations between the tracer position and the occupation of the site ahead, whose contribution becomes dominant when the bias experienced by the tracer is large enough. We finally show that our decoupling scheme becomes exact in both the high- and low-density limits, which validates its relevance.

P. I. acknowledges financial support from the U.S. National Science Foundation under MRSEC Grant No. DMR-1420620. The work of O. B. is supported by the European Research Council (Grant No. FPTOpt-277998).

*Present address: ESPCI Paris, PSL Research University, UMR Gulliver 7083, 10 rue Vauquelin, 75005 Paris, France.

[1] F. Höfling and T. Franosch, Rep. Prog. Phys. **76**, 046602 (2013).
[2] T. Chou, K. Mallick, and R. K. P. Zia, Rep. Prog. Phys. **74**, 116601 (2011).
[3] C. Bechinger, R. Di Leonardo, H. Löwen, C. Reichhardt, G. Volpe, and G. Volpe, Rev. Mod. Phys. **88**, 045006 (2016).
[4] P. Illien, R. Golestanian, and A. Sen, Chem. Soc. Rev. **46**, 5508 (2017).
[5] L. G. Wilson and W. C. K. Poon, Phys. Chem. Chem. Phys. **13**, 10617 (2011).
[6] R. P. A. Dullens and C. Bechinger, Phys. Rev. Lett. **107**, 138301 (2011).
[7] A. M. Puertas and T. Voigtmann, J. Phys. Condens. Matter **26**, 243101 (2014).
[8] C. Mejia-Monasterio and G. Oshanin, Soft Matter **7**, 993 (2011).
[9] H. Tanaka, A. A. Lee, and M. P. Brenner, Phys. Rev. Fluids **2**, 043103 (2017).
[10] S. N. Weber, C. A. Weber, and E. Frey, Phys. Rev. Lett. **116**, 058301 (2016).
[11] J. Stenhammar, R. Wittkowski, D. Marenduzzo, and M. E. Cates, Phys. Rev. Lett. **114**, 018301 (2015).
[12] V. Démery, Phys. Rev. E **91**, 062301 (2015).
[13] V. Démery, O. Bénichou, and H. Jacquin, New J. Phys. **16**, 053032 (2014).
[14] K. Mallick, Physica (Amsterdam) **418A**, 17 (2015).
[15] O. Bénichou, A. M. Cazabat, J. De Coninck, M. Moreau, and G. Oshanin, Phys. Rev. Lett. **84**, 511 (2000).
[16] O. Bénichou, A. M. Cazabat, J. De Coninck, M. Moreau, and G. Oshanin, Phys. Rev. B **63**, 235413 (2001).
[17] S. Leitmann and T. Franosch, Phys. Rev. Lett. **111**, 190603 (2013).
[18] O. Bénichou, P. Illien, G. Oshanin, A. Sarracino, and R. Voituriez, Phys. Rev. E **93**, 032128 (2016).
[19] S. Leitmann and T. Franosch, Phys. Rev. Lett. **118**, 018001 (2017).
[20] O. Bénichou, A. Bodrova, D. Chakraborty, P. Illien, A. Law, C. Mejía-Monasterio, G. Oshanin, and R. Voituriez, Phys. Rev. Lett. **111**, 260601 (2013).
[21] D. Winter, J. Horbach, P. Virnau, and K. Binder, Phys. Rev. Lett. **108**, 028303 (2012).
[22] C. F. E. Schroer and A. Heuer, Phys. Rev. Lett. **110**, 067801 (2013).
[23] P. Reimann, C. Van den Broeck, H. Linke, P. Hänggi, J. M. Rubi, and A. Pérez-Madrid, Phys. Rev. Lett. **87**, 010602 (2001).
[24] K. Lindenberg, A. M. Lacasta, J. M. Sancho, and A. H. Romero, New J. Phys. **7**, 29 (2005).
[25] B. Lindner and I. M. Sokolov, Phys. Rev. E **93**, 042106 (2016).
[26] P. Reimann and R. Eichhorn, Phys. Rev. Lett. **101**, 180601 (2008).
[27] B. Lindner and E. M. Nicola, Phys. Rev. Lett. **101**, 190603 (2008).
[28] K. Nakazato and K. Kitahara, Prog. Theor. Phys. **64**, 2261 (1980).
[29] See Supplemental Material at http://link.aps.org/supplemental/10.1103/PhysRevLett.120.200606 for details on the analytical approach.

[30] O. Bénichou, P. Illien, G. Oshanin, A. Sarracino, and R. Voituriez, Phys. Rev. Lett. **113**, 268002 (2014).
[31] P. Illien, O. Bénichou, G. Oshanin, and R. Voituriez, J. Stat. Mech. (2015) P11016.
[32] B. D. Hughes, *Random Walks and Random Environments: Random Walks*, Vol. 1 (Oxford University Press, Oxford, 1995).
[33] We checked numerically that $D(F)$ is decreasing even for $\rho = 0.1$ and $\tau^* = 10$, but too slowly to be shown with this scale.
[34] P. Baerts, U. Basu, C. Maes, and S. Safaverdi, Phys. Rev. E **88**, 052109 (2013).
[35] M. J. A. M. Brummelhuis and H. J. Hilhorst, J. Stat. Phys. **53**, 249 (1988).
[36] M. J. A. M. Brummelhuis and H. J. Hilhorst, Physica (Amsterdam) **156A**, 575 (1989).
[37] O. Bénichou and G. Oshanin, Phys. Rev. E **66**, 031101 (2002).